Kinetics and Mechanisms of Reactions of Methyldioxorhenium(V) in Aqueous Solutions: Dimer Formation and Oxygen-Atom Abstraction Reactions

James H. Espenson* and Douglas Tak Yeung Yiu†

Ames Laboratory and Department of Chemistry, Iowa State University, Ames, Iowa 50011

Received February 7, 2000

The stable compound CH_3ReO_3 (MTO), upon treatment with aqueous hypophosphorous acid, forms a colorless metastable species designated MDO, $CH_3ReO_2(H_2O)_n$ ($n = 2$). After standing, MDO is first converted to a yellow dimer ($\lambda_{max} = 348$ nm; $\epsilon = 1.3 \times 10^4$ L mol^{-1} cm^{-1}). That reaction follows second-order kinetics with $k = 1.4$ L mol^{-1} s^{-1} in 0.1 M aq trifluoromethane sulfonic acid at 298 K. Kinetics studies as functions of temperature gave $\Delta S^{\ddagger} = -4 \pm 15$ J K^{-1} mol^{-1} and $\Delta H^{\ddagger} = 71.0 \pm 4.6$ kJ mol^{-1}. A much more negative value of $\Delta S^{\ddagger}$ would be expected for simple dimerization, suggesting the release of one or more molecules of water in forming the transition state. If solutions of the dimer are left for a longer period, an intense blue color results, followed by precipitation of a compound that does, even after a long time, retain the Re−CH_3 bond in that aq. hydrogen peroxide generates the independently known $CH_3Re(O)(O_2)_2(H_2O)$. The blue compound may be analogous to the intensely colored purple cation $[(Cp^*Re)_3(\mu_2\text{-}O)_3(\mu_3\text{-}O)_3ReO_3]^+$. If a pyridine *N*-oxide is added to the solution of the dimer, it is rapidly but not instantaneously lost at the same time that a catalytic cycle, separately monitored by NMR, converts the bulk of the PyO to Py according to this stoichiometric equation in which MDO is the active intermediate: $C_5H_5NO + H_3PO_2 \rightarrow C_5H_5N + H_3PO_3$. A thorough kinetic study and the analysis by mathematical and numerical simulations show that the key step is the conversion of the dimer **D** into a related species **D*** (presumably one of the two μ-oxo bonds has been broken); the rate constant is 5.6×10^{-3} s^{-1}. **D*** then reacts with PyO just as rapidly as MDO does. This scheme is able to account for the kinetics and other results.

Introduction

The chemistry of hydrated methyldioxorhenium(V) in solution continues to reveal new features. The original discovery of CH_3ReO_2 in aqueous solution stems from the reduction of CH_3ReO_3 by H_3PO_2.[1] We presume that the resulting species exists in water as the diaqua $CH_3ReO_2(H_2O)_2$, as shown in Chart 1, although specific proof of the degree of hydration is lacking. A useful abbreviation for it is MDO.[1−3] We suggest that MDO contains five-coordinate rhenium, based on compounds such as $CH_3ReO_2(PPh_3)_2$,[4,5] CH_3ReO(dithiolate)L (dithiolate is the anion of 2-mercaptomethylthiophenol; L = phosphine, pyridine, etc.),[6,7] and $CH_3Re(NAr)_2(PMe_2Ph)_2$ (Ar = 2,6-diisopropylphenyl).[8] MDO is metastable,[1] first forming a dimer (**D**) (which is the subject of this investigation) and then, more slowly, a deep blue insoluble oligomer, possibly related to the tetrarhenium cation derived from Cp^*ReO_2,[9] also shown in Chart 1. Further comments on the structure and composition of MDO will be made later.

These are the subjects we address in this work: (1) the kinetics and mechanism of the dimerization of MDO, including a determination of the activation parameters for this uncommon reaction; (2) reactions of **D** with oxo-donor reagents, especially pyridine *N*-oxides, that cause it to revert to MDO; and (3) the multistep catalytic processes that allow a trace concentration of Re(V) to convert pyridine *N*-oxides catalytically to pyridines, with hypophosphorous acid serving as the stoichiometric source of oxygen. The complex kinetic data were examined in terms of several reaction schemes to determine which data were consistent with the observations. The net reaction that occurs in the catalytic cycle is

$$C_5H_5NO + H_3PO_2 \rightarrow C_5H_5N + H_3PO_3 \qquad (1)$$

Experimental Section

Materials. High-purity water was obtained by passing laboratory-distilled water through a Millipore-Q water purification system. Methyltrioxorhenium was prepared according to the literature procedure.[10] Hypophosphorous acid was the commercial 50% reagent. Trifluoromethanesulfonic acid, obtained as a material of 98% purity, was diluted with water and standardized against potassium hydrogen phthalate. The pyridine oxides were purchased. Their concentrations in these experiments were determined from the spectra in aqueous solution with the values of ϵ_{256} (10^4 L mol^{-1} cm^{-1}) obtained in this work: 4-MePyO, 1.43;[11] PyO, 1.19;[11] 2-MePy, 0.69.

* Corresponding author. E-mail: espenson@iastate.edu.
† On leave from City University of Hong Kong.

(1) Abu-Omar, M. M.; Appleman, E. H.; Espenson, J. H. *Inorg. Chem.* **1996**, *35*, 7751−7757.
(2) Abu-Omar, M. M.; Espenson, J. H. *Inorg. Chem.* **1995**, *34*, 6239−6240.
(3) Lahti, D. W.; Espenson, J. H. *Inorg. Chem.* **1999**, *38*, 5230−5234.
(4) Herrmann, W. A.; Roesky, P. W.; Wang, M.; Scherer, W. *Organometallics* **1994**, *13*, 4531−4535.
(5) Eager, M. D.; Espenson, J. H. *Inorg. Chem.* **1999**, *38*, 2533−2535.
(6) Jacob, J.; Guzei, I.; Espenson, J. H. *Inorg. Chem.* **1999**, *39*, 1040−1041.
(7) Jacob, J.; Guzei, I.; Espenson, J. H. *Inorg. Chem.* **1999**, *38*, 3266−3267.
(8) Wang, W.-D.; Espenson, J. H. Submitted for publication.
(9) Gable, K. P.; Juliette, J. J. J.; Gartman, M. A. *Organometallics* **1995**, *14*, 3138−3140.
(10) Herrmann, W. A.; Kratzer, R. M.; Fischer, R. W. *Angew. Chem., Int. Ed. Engl.* **1997**, *36*, 2652−2654.
(11) Jaffe, H. H. *J. Am. Chem. Soc.* **1955**, *77*, 4451.

10.1021/ic000128h CCC: $19.00
Published on Web 08/10/2000

Chart 1. Selected Oxorhenium(V) Compounds

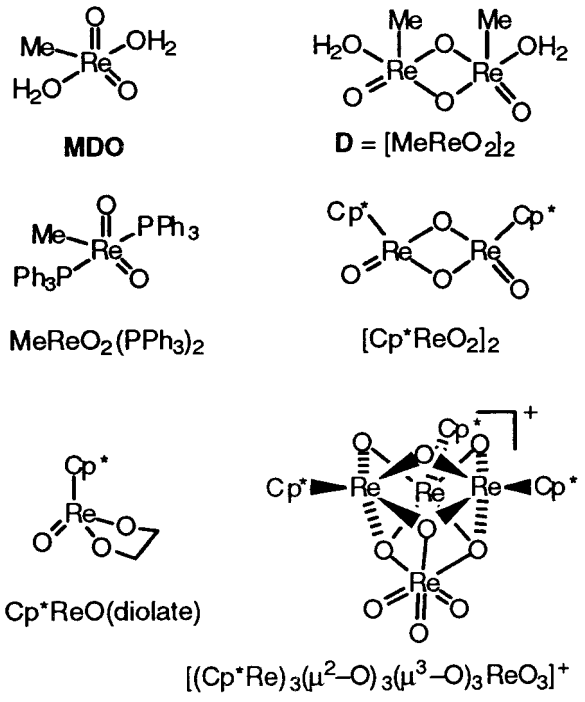

Reaction Kinetics. The reactions of PyO in this system were studied in aqueous solution, for the most part spectrophotometrically. MDO was generated from 0.27−0.80 mM MTO with 0.80 M (usually) H_3PO_2 in solutions containing 0.10 M HOTf, added to maintain the stability of this compound.[1] MDO does not have any useful UV−vis or NMR spectrum, whereas **D** does. As determined in the course of this research, the most useful absorption band occurs at 348 nm ($\epsilon = 1.3 \times 10^4$ L mol^{-1} cm^{-1}). The spectrophotometric experiments on the formation of **D** and its subsequent reactions were carried out at this wavelength. A few reactions were carried out by ^{1}H NMR to follow the loss of PyO and the buildup of PyD^+. The solvent was D_2O, and the concentrations were the same as those used in the more numerous UV−vis determinations.

Results

Dimerization of $MeReO_2$. MDO was generated in aqueous solution from the reaction of MTO with hypophosphorous acid according to

$$CH_3ReO_3 + H_3PO_2 + 2H_2O \rightarrow CH_3ReO_2(H_2O)_2 + H_3PO_3 \quad (2)$$

The rate constant for this reaction in aqueous solution is 2.8×10^{-2} L mol^{-1} s^{-1} at 25.0 °C.[1] In these and other experiments, a high concentration of H_3PO_2 was used, usually 0.8 M. Under these conditions, therefore, reaction 2, with $t_{1/2} = 31$ s, is far more rapid than dimerization.

When solutions of MDO are allowed to stand, certain reactions occur in sequence. First, the yellow-colored dimeric Re(V) species, **D**, is formed

$$2CH_3ReO_2(H_2O)_2\,(\text{MDO}) \rightarrow \mathbf{D} + nH_2O \quad (3)$$

At longer times, without interfering in the study of dimerization, further spectroscopic changes were noted that can be attributed to the conversion of **D** to an oligomeric form of MDO. During those latter stages, the solution developed an intense blue coloration, following which a gelatinous dark-blue precipitate formed. The addition of excess hydrogen peroxide quantitatively restored $CH_3Re(O)(\eta^2\text{-}O_2)_2H_2O$, the same species formed from

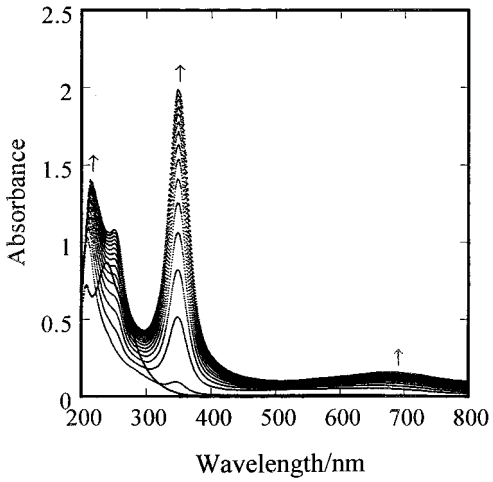

Figure 1. Repetitive scan experiment using these concentrations in aqueous solution at 25.0 °C: 0.38 mM CH_3ReO_3, 800 M H_3PO_2, and 0.1 M CF_3SO_3H. The graph shows 15 spectra taken at 300 s intervals. The first spectrum (heavier line) shows CH_3ReO_3 prior to reduction. The rate-controlling process is the dimerization of $CH_3ReO_2(H_2O)_2$.

CH_3ReO_3 and excess H_2O_2.[1] The clear implication is that the CH_3−Re bond, despite its occasional fragility toward base hydrolysis,[12] remains intact.

Because this study concerns oxorhenium(V) compounds that are not amenable to direct structural characterization, we have relied on a considerable number of close and distant analogues in postulating likely compositions and structures. As to the monomeric MDO, it must be a hydrated species providing at least five ligands for coordination to Re(V). This solid compound has been characterized: $MeReO_2(PPh_3)_2 \cdot MeReO_3$; in it, the Re(V) center is five-coordinated with trans-disposed phosphine ligands.[4] Another related monomer is Cp*ReO(diolate), one example of which is shown in Chart 1.[13,14] We note also the five-coordinate Re(V) in MeReO(mtp)L ($mtpH_2$ = 2-mercaptomethylthiophenol; L = Py, PR_3).[6,7] The Cp^*ReO_2 monomer appears not to have been prepared,[9] but $[Cp^*ReO_2]_2$ has been characterized.[9,15−17]

Our initial subject is the dimerization of MDO. The UV−visible spectrum was scanned at 300 s intervals, as displayed in Figure 1. It clearly shows the development of distinct spectroscopic features of the yellow-colored compound **D**. An additional, long-wavelength peak near 670 nm develops at longer times; eventually, this deeply colored blue species will attain a high absorbance. It represents the beginning of oligomer formation and may be analogous to the intensely colored purple cation $[(Cp^*Re)_3(\mu_2\text{-}O)_3(\mu^3\text{-}O)_3ReO_3]^+$,[9] shown in Chart 1, and $\{[(tacn)ReO)]_2(\mu\text{-}O)_2\}^{2+}$.[18]

Kinetics experiments on the dimerization step were monitored through the growth of absorbance at the 348 nm maximum of **D**. Single-wavelength kinetics determinations were carried out over a range of initial concentrations of MTO, 0.27−0.80 mM at 348 nm, monitoring the buildup of **D**, which has a molar

(12) Abu-Omar, M.; Hansen, P. J.; Espenson, J. H. *J. Am. Chem. Soc.* **1996**, *118*, 4966−4974.
(13) Herrmann, W. A.; Herdtweck, E.; Floel, M.; Kulpe, J.; Kusthardt, U.; Okuda, J. *Polyhedron* **1987**, *6*, 1165−1182.
(14) Gable, K. P.; Phan, T. N. *J. Am. Chem. Soc.* **1994**, *116*, 833−839.
(15) Herrmann, W. A.; Flöel, M.; Kulpe, J.; Felixberger, J.; Herdtweck, E. *J. Organomet. Chem.* **1988**, *355*, 297−313.
(16) Herrmann, W. A.; Serrano, R.; Küsthardt, U.; Ziegler, M. L.; Guggolz, E.; Zahn, T. *Angew. Chem., Int. Ed. Engl.* **1984**, *23*, 515−517.
(17) Herrmann, W. A.; Serrano, R.; Küsthardt, U.; Guggolz, E.; Nuber, B.; Ziegler, M. *J. Organomet. Chem.* **1985**, *287*, 329−344.
(18) Conry, R. R.; Mayer, J. M. *Inorg. Chem.* **1990**, *29*, 4862−4867.

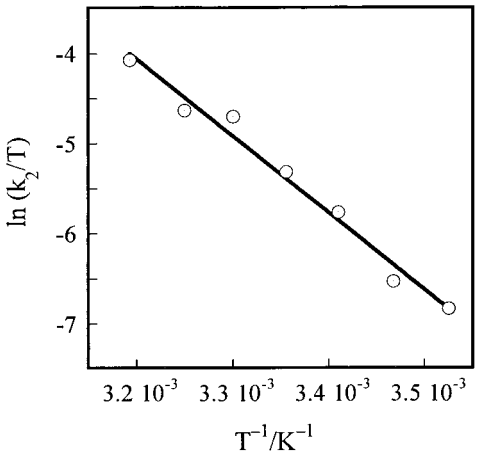

Figure 2. Analysis of the temperature dependence of the rate constant for the dimerization of $CH_3ReO_2(H_2O)_2$ according to the Eyring equation (eq 5).

absorptivity designated ϵ_D. This gives the values of $[MDO]_t$ as $[MDO]_0 - 2[\mathbf{D}]_t$. The reaction has a second-order rate law

$$-\frac{d[MDO]}{dt} = k[MDO]^2 = 2\frac{d[D]}{dt} \qquad (4)$$

The fit of the data gave $k = 1.4 \pm 0.2$ L mol^{-1} s^{-1} at 25.0 °C and $\epsilon_D = (1.32 \pm 0.11) \times 10^4$ L mol^{-1} cm^{-1} at 348 nm.

Activation Parameters. Similar experiments were carried out at seven different temperatures in the range of 10−40 °C. These are the values obtained: $T = 10.7$, 15.4, 20.3, 25.0, 30.0, 34.7, and 40.2 °C, corresponding to k values of 0.30_6, 0.42, 0.92, 1.3, 2.75, 3.01, and 5.33 L mol^{-1} s^{-1}, respectively.

Activation parameters were obtained by a least-squares fittings of the data to the Eyring equation (eq 5), resulting in $\Delta S^{\ddagger} = -4 \pm 15$ J K^{-1} mol^{-1} and $\Delta H^{\ddagger} = 71.0 \pm 4.6$ kJ mol^{-1} (see Figure 2).

$$k = \frac{k_B T}{h} \exp\left(-\frac{\Delta H^{\ddagger}}{RT}\right) \exp\left(\frac{\Delta S^{\ddagger}}{R}\right) \qquad (5)$$

Reactions with Pyridine *N*-Oxides. Given that MDO is a reagent for oxygen-atom abstraction, it seemed worthwhile to test **D** for that possibility. We have studied pyridine *N*-oxide, 4-Me-pyridine *N*-oxide, and 2-Me-pyridine *N*-oxide (all designated as PyO in general), which are known to react rapidly with MDO according to

$$CH_3ReO_2(H_2O)_2 + PyO \rightarrow CH_3ReO_3 + Py + 2H_2O \qquad (6)$$

The rate constants are 4.60×10^3 L mol^{-1} s^{-1} for C_5H_5NO and 7.10×10^3 L mol^{-1} s^{-1} for 4-MeC_5H_4NO at 25 °C.[1] To conduct the experiments with **D**, we injected PyO into the solution at a selected point during the buildup of **D**. In doing that, rather than waiting until formation of **D** was complete, we minimized possible interference from the oligomers formed later. The "initial" (relative to the start of the new reaction) concentration of **D** was calculated accurately from its molar absorptivity.

Once pyridine oxide had been added, however, the buildup of **D** reversed the reaction course, and the absorbance gradually fell to a small value. In a third stage, the absorbance suddenly began to rise, as the dimerization of MDO began again, signaling the precise moment when all the pyridine *N*-oxide had been consumed. The absorbance−time profile for one set of such reactions is given in Figure 3. During the consumption of **D**

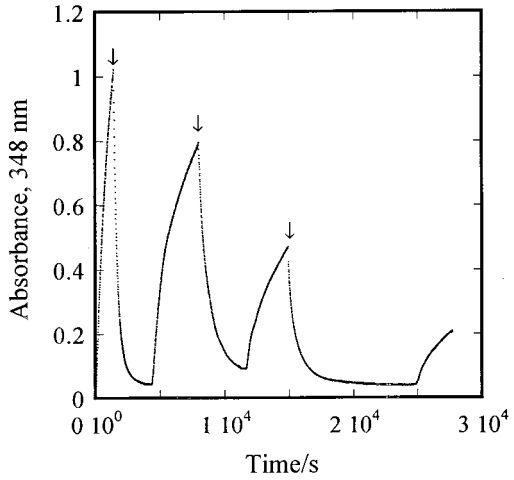

Figure 3. Rising absorbance as $CH_3ReO_2(H_2O)_2$ converts to the dimer **D** is interrupted upon the addition of 4-MeC_5H_4NO. The concentration of **D** then decreases until 4-MeC_5H_4NO has been depleted. Following that, dimerization resumes again. The points at which Py was injected (24, 24, and 48 mM) are shown with arrows. The experiments were carried out in aqueous solution with 800 mM H_3PO_2 and 0.1 M CF_3SO_3H.

and for a period thereafter, a catalytic sequence (reactions 2 and 6 in tandem) takes place. With $[H_3PO_2] = 0.4$ M, half the previous value, the concentration of **D** remains at zero for a longer time before its sudden rise, since the catalytic cycle is that much slower. The formation of **D** takes place only after the concentration of PyO, limiting in the sense of the overall stoichiometry of eq 1, has been exhausted.

If **D** and PyO react directly, then the rate constant, roughly 1 L mol^{-1} s^{-1}, is considerably smaller than k for MDO and PyO, ~10^3 L mol^{-1} s^{-1}. This formulation will not be pursued, however, for later analysis showed that **D** and PyO do not react ($k \ll 10^{-2}$ L mol^{-1} s^{-1}).

The kinetic data during the stage in which **D** declines in concentration were analyzed by the initial rate method with a polynomial fit, first converting absorbances into [**D**].[19] Depending on the time along the rising curve of **D** at which PyO was injected, the experiment provided a different initial concentration of **D**. The reaction was first-order with respect to [**D**] at constant [PyO] over a substantial concentration range. Representative data, depicted in Figure 4, show this relation. This direct dependence of rate on [**D**] allowed us to rule out one credible mechanism, to be cited later.

The dependence of the initial rate upon the concentration of each pyridine *N*-oxide is more complex. The initial rate can be expressed by

$$v_i = \frac{k\,[\mathbf{D}]\,[PyO]}{\kappa + [PyO]} \qquad (7)$$

Rearrangement to a linearized form is possible

$$\frac{[\mathbf{D}]}{v_i} = \frac{\kappa}{k}\frac{1}{[PyO]} + \frac{1}{k} \qquad (8)$$

Figure 5 shows the plots of $[\mathbf{D}]/v_i$ against 1/[PyO], which are indeed linear. The values of parameter $k/10^{-3}$ s^{-1} are 5.60 ± 0.22, 5.59 ± 0.36, and ca. 4 for C_5H_5NO, 4-$CH_3C_5H_4NO$, and 2-$CH_3C_5H_4NO$, respectively, and the values of $\kappa/10^{-3}$ mol L^{-1}

(19) Hall, K. J.; Quickenden, T. I.; Watts, D. W. *J. Chem. Educ.* **1976**, *53*, 493.

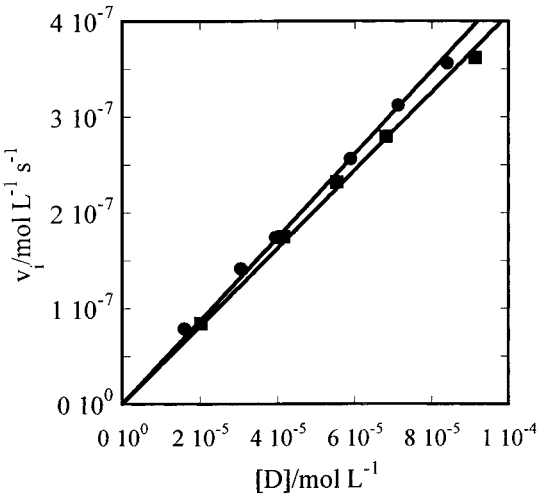

Figure 4. Linear dependence of the initial rate (in aqueous solution containing 0.1 M CF_3SO_3H at 25.0 °C) against $[\mathbf{D}]_0$ in two groups of experiments with 25 mM pyridine *N*-oxide (circles) and 20 mM 4-methylpyridine *N*-oxide (squares).

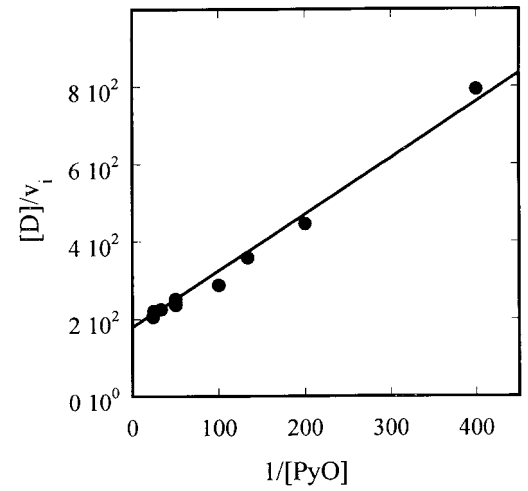

Figure 5. Dependence of the initial rate on [PyO] in systems containing PyO and the MDO dimer **D** in 0.10 M aq HOTf at 25.0 °C. Data are represented by a plot of $[\mathbf{D}]/v_i$ against 1/[PyO].

for the complexes are 6.7 ± 0.9, 7.22 ± 0.66, and ca. 60, respectively.

It can be seen that the value of k is approximately the same for two compounds. (The resolution of the values of v_i into k and κ for 2-$CH_3C_5H_4NO$, on the other hand, was poor, since the larger value of κ would have required a higher [PyO] than allowed.) The value of κ, on the other hand, varies from case to case. These findings are important for a consistent mechanism, as taken up in the Discussion. Another point of significance can be seen from Figure 3: the absorbance does not vary at the point where PyO was injected. That was true for every such experiment.

A few experiments were carried out with Me_2SO in place of PyO. The absorbance of **D** gradually but more slowly decreases with addition of the sulfoxide, but it does not rise again. As an independent experiment, Me_2SO was added to a solution of MDO in which **D** had formed in about half the concentration it would ultimately attain. At that point, the absorbance remained constant, and the formation of **D** was permanently interrupted. Evidently, MDO and Me_2S form a tight complex. This will account for all of these observations. As precedent for that, we note much recent evidence for Re(V)−thiolate and thio complexes.[6,7] In addition, oxorhenium(V) compounds are known

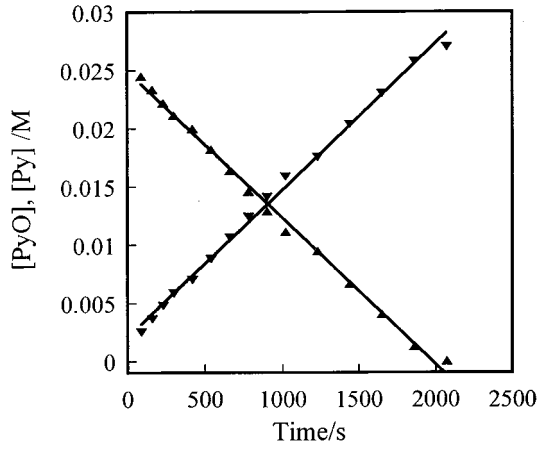

Figure 6. Concentrations of PyO and PyH^+, analyzed by ^1H NMR, follow zero-order kinetics in reactions with MTO (0.4 mM), $H_2P(O)$-OD (800 mM), and 4-MeC_5H_4NO (27 mM) in D_2O containing 0.1 M CF_3SO_3D at 25.0 °C. Each line has a slope of 1.30×10^{-5} mol L^{-1} s^{-1}.

to serve as catalysts for O-atom transfer from R_2SO, showing rate inhibition by R_2S.[20]

NMR Experiments. Because the spectrophotometric method allows only **D** to be followed uniquely, we turned to ^1H NMR in monitoring the CH_3 singlets of 4-C$H_3C_5H_4NO$ and 4-C$H_3C_5H_4$-ND^+ in D_2O. Figure 6 shows the result of such an experiment. It confirms that PyO is quantitatively converted to Py (actually, PyD^+ under these conditions), as anticipated when reaction 1 is the net result of using hypophosphorous acid in excess over PyO. The conversion follows zero-order kinetics, consistent with the known[1] catalytic conversion cycle with eq 1 as the resultant.

In the interpretation of these data, we determined the rate constant for the reaction of MTO with partially deuterated hypophosphorous acid in D_2O. This was done spectrophotometrically, following the loss of MTO absorbance at 270 nm ($\epsilon = 1.3 \times 10^3$ L mol^{-1} cm^{-1}). The rate constant so determined was $k_1 = 5.5 \times 10^{-2}$ L mol^{-1} s^{-1} (cf. the 3.9×10^{-2} L mol^{-1} s^{-1} given earlier).[1] This value was needed for the kinetic analysis; the issue of the inverse kinetic isotope effect on k_1 has been dealt with earlier.[1]

Discussion

Dimerization of MDO. The second-order kinetics confirms the hypothesis that dimer formation requires a bimolecular step. The activation parameters, however, are surprising, particularly $\Delta S^{\ddagger}$, since bimolecular combination reactions are inevitably accompanied by a large decrease in activation entropy even when no net association results. We suggest that a compensating factor in this particular case is the positive contribution to $\Delta S^{\ddagger}$ from the release of coordinated water molecules during the activation process (eq 2). The magnitude must be quite substantial to offset the inherently negative $\Delta S^{\ddagger}$ for pure dimerization.

Insofar as the kinetic and spectrophotometric data showed, the dimerization of MDO proceeded to completion, even at the lowest concentration. A conservative limit on the equilibrium constant for reaction 3 is $K_3 > 10^7$, or $\Delta G_3^{\circ} < -40$ kJ at 298 K. A value of that magnitude does not entirely preclude a step in the mechanism in which **D** reverts to 2 MDO, a point we add in anticipation of one proposal concerning the mechanism.

Oxo Transfer. The three reaction schemes in Scheme 1 are potentially consistent with the kinetic data. In the first, A, a

(20) Abu-Omar, M. M.; Khan, S. I. *Inorg. Chem.* **1998**, *37*, 4979−4985.

Scheme 1. Tentative Reaction Schemes

Common steps: $MTO + H_3PO_2 \rightarrow MDO + H_3PO_3$ [k_1]

$MDO + PyO \rightarrow MTO + Py$ [k_3]

Individual steps and reaction schemes:

A	*B*	*C*
$2\,MDO \rightarrow D$ [k_2]	$2\,MDO \rightarrow D$ [k_2]	$2MDO \rightleftarrows D$ [k_2, k_{-2}]
$D + PyO \rightleftharpoons D\text{-}OPy$ [K]	$D \rightleftarrows D^*$ [k_4, k_{-4}]	
$D\text{-}OPy \rightarrow MTO + MDO + Py$ [k_6]	$D^* + PyO \rightarrow MTO + MDO + Py$ [k_5]	

Derived rate equations for loss of **D**, v =

$$\frac{k_6[\mathbf{D}]\cdot[PyO]}{K^{-1}+[PyO]} \qquad \frac{k_4[\mathbf{D}]\cdot[PyO]}{\frac{k_{-4}}{k_5}+[PyO]} \qquad \frac{2k_{-2}k_3[\mathbf{D}]\cdot[PyO]}{\frac{1}{3}\sqrt{k_3[PyO]+16k_2k_{-2}[\mathbf{D}]}+[PyO]}$$

Scheme 2

$$2\,MDO \underset{k_{-2}}{\overset{k_2}{\rightleftharpoons}} D^* \underset{k_4}{\overset{k_{-4}}{\rightleftharpoons}} D$$

prior equilibrium is proposed between **D** and PyO. In B, a steady-state scheme, **D** rearranges to form **D***, which is evidently much more active in the oxo-transfer step than **D** itself. In C, the formation of **D** from MDO is postulated to be sufficiently reversible, allowing **D** to regenerate MDO, known to react rapidly with PyO. The rate law is given for each of the proposals.

Reaction schemes A and C can be eliminated by the following analysis. The saturation of the pre-equilibrium proposed in A would lead to a distribution between **D** and **D**-OPy, yet the absorbance of **D** did not perceptibly vary upon addition of PyO. Scheme C lacks the precise kinetic form needed, but it is close enough that an analysis is warranted. C fails on two other counts: the order with respect to **D** remains at unity (see Figure 4) over a wide concentration range, and in the numerical fitting, no real number could be found for k_{-2} with k_2 and k_3 set at their known values. Both points contradict C.

Mechanistic Analysis. We therefore begin an analysis of mechanism B. If this mechanism is to account for the various observations, then intermediate **D*** must be involved in two instances, as shown not only with PyO in Scheme 1, but also in the conversion of MDO to **D** given in Scheme 2. In neither experiment does **D*** attain a detectable concentration level. Given the sense of the dimerization process, it seems plausible that **D*** is a half-bonded (half-opened) version of **D**.

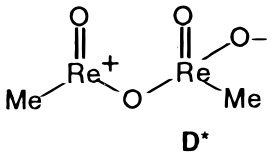

D*

In that sense, **D*** is much like the monodentate intermediate that lies between a metal complex ML_6 and the chelated product of its reaction with a bidentate ligand. As in that analogy, the experimental rate constant is evidently that for the first substitution step, the chelate closure being much more rapid.

The overall conversion of MDO to **D** proceeds to completion, based on the constant molar absorptivity of the product at all starting concentrations. One can therefore set a limit on the equilibrium constant and then on the component rate constants. From the preceding equation we have, conservatively

$$K = \frac{\overline{[\mathbf{D}]}}{\overline{[MDO]^2}} = \frac{k_2k_{-4}}{k_{-2}k_4} > \sim 10^7 \qquad (9)$$

With the known values of k_2 and k_4, we then obtain

$$\frac{k_{-4}}{k_{-2}} = K\frac{k_4}{k_2} = (>10^7)\,\frac{5.6\times10^{-3}}{1.4} \geq 4\times10^3 \qquad (10)$$

For this scheme to agree with the data, it also is necessary that **D*** reacts preferentially with PyO, rather than converting into 2 MDO. Thus, this inequality can be written

$$K_{-2} \gg k_5[PyO] \qquad (11)$$

If the experimental result for 4-MePyO, $k_{-4}/k_5 = 7.2\times10^{-3}$ mol L^{-1}, were incorporated, then at 4×10^{-2} mol L^{-1} PyO, a typically high concentration, $k_{-4} \gg 0.2k_{-2}$ would be obtained. Although a less strict limitation, this is consistent with eq 10.

A shakier extension of this analysis is to suggest that k_5 might have a value similar to that of k_3, given the suggested similarity in structure. If so, then the approximate values are $k_{-4} \approx 30-50\ s^{-1}$ and (from eq 10) $k_{-2} \approx 10^{-3}\ s^{-1}$. These numbers are necessarily consistent with the limit of *K* under the method used. Table 1 presents the experimental and estimated rate constants.

Incidentally, if the rate constants for the reactions in Scheme 2 are examined, it is clear that MDO and **D*** equilibrate much more slowly than **D*** and **D** do. This is consistent with the lack of accumulation of **D*** and with the loose analogy drawn between these two reactions and stepwise chelate formation, where the ring closing step is invariably more rapid than bimolecular substitution. As to why the reactions take place as **D** → **D*** (k_4) rather than **D** → 2 MDO (k_{-2}), we note that the k_{-2} step poses a significant barrier for the latter. It seems that **D*** has an MDO-like center and, as a result, will be highly reactive with PyO. Since **D*** must almost certainly lie on the pathway between MDO and **D**, Scheme 2 follows as a consequence of the acceptance of mechanism B.

Numerical Simulations. The steady-state reaction sequence B fits the mathematical requirements, including the observation that the intermediate **D*** does not build up to a detectable concentration. Owing to the complexity of this scheme, it was also examined with kinetics simulation techniques, for which the program KinSim was used.[21−24] Particular emphasis was

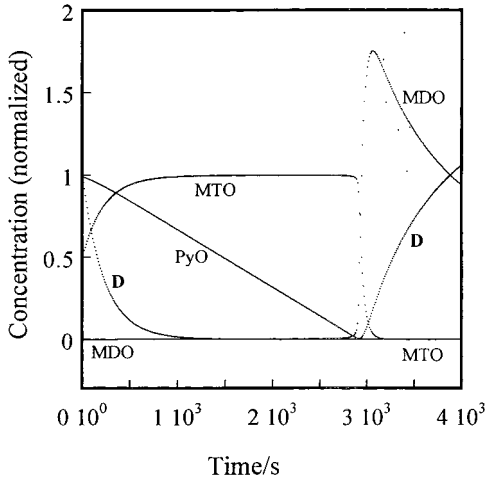

Figure 7. Concentrations of the indicated compounds, each normalized via division by its initial or final concentration. The initial concentrations for the simulation were 0.80 M H_3PO_2, 25 mM 4-MeC_5H_4NO, 0.10 mM **D**, and 0.20 mM MDO.

Table 1. Summary of Experimental and Estimated (in parentheses) Rate Constants

reaction	k[a] at 25 °C	source
$MTO + H_2PO_2^- \rightarrow MDO + H_3PO_3$	$k_1 = 2.8 \times 10^{-2}$	ref 1
$2\ MDO \underset{k_{-2}}{\overset{k_2}{\rightleftharpoons}} \mathbf{D}^*$	$k_2 = 1.4$ ($k_{-2} < \sim 10^{-2}$)	this work
$MDO + XC_5H_4NO \rightarrow MTO + XC_5C_4N$	$k_3 = 7.1 \times 10^3$ (X = 4-Me), 4.6×10^3 (X = H)	ref 1
$D^* \underset{k_4}{\overset{k_{-4}}{\rightleftharpoons}} \mathbf{D}$	($k_{-4} \approx 30-50$) $k_4 = 5.6 \times 10^{-3}$	this work
$\mathbf{D}^* + XC_5H_4NO \rightarrow MTO + MTO + XC_5H_4N$	($k_5 \approx k_3$ assumed)[b] $k_{-4}/k_5 = 7.2 \times 10^3$ (X = 4-Me), 6.7×10^3 (X = H)	this work

[a] With mol L^{-1} and s as the units for concentration and time, respectively. [b] See text.

placed on examining [**D**] as the computed output, since **D** is the principal observable product in the experiments. In the simulations, the rate constants in Table 1 were used for the results, but many other combinations were tested to probe the stability of this set. Two are displayed in Figure 7: the concentrations (normalized for purposes of display) of MTO, MDO, **D**, and PyO as functions of time; and (separately) the Py that arises from eqs 3 and 5.

The concordance of this model with the experimental data should be noted. The concentration of **D** decreases upon the injection of PyO at a simulated rate, in agreement with eq 7. It attains a minimum level governed by [PyO]; if [PyO] is greater, then $[\mathbf{D}]_{min}$ is essentially zero, and it remains at that level for times that are longer at higher [PyO]. Concurrent with those optically monitored events, [PyO] decreases as [Py] increases catalytically via the sequential operation of the reactions given at the top of Scheme 1. In agreement with the experimental NMR findings (Figure 6), the catalytic decrease of PyO and the buildup of Py follow zero-order kinetics. Under these conditions, much of the consumption of PyO arises from the MDO cycle, but relatively little results from the sequence with **D**. At the point when PyO has been exhausted, the formation of **D** resumes its course. As can be seen from Figure 3, that is often an abrupt change. This is a clock reaction in that MDO, in competition with its rapid (k_3) consumption by PyO, cannot survive to begin the buildup of **D**; only when PyO has been exhausted can reaction 3 recommence.

Detailed mechanistic speculation is hardly warranted, given the tentative nature of some structural assignments. Nonetheless, it is useful to imagine the molecular process by which **D*** and PyO react. In that step, cleavage of the N−O bond of PyO must provide a rate-controlling barrier. The possible structure of the transition state shows that electronic flow from one end of the molecule to the other leads to the smooth conversion of reactants to products, as depicted here.

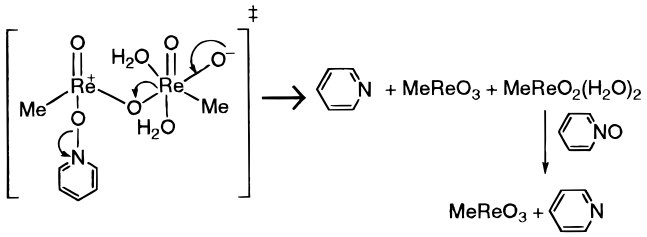

Acknowledgment. This research was supported by a grant from the National Science Foundation. Some experiments were conducted at the facilities of the Ames Laboratory. The authors thank A. Bakac, D. W. Lahti, G. Lente, and X. Shan for assistance and discussions. D.T.Y.Y. acknowledges the support of the City University Hong Kong while he was at Iowa State University.

IC000128H

(21) Barshop, B. A.; Wrenn, C. F.; Frieden, C. *Anal. Biochem.* **1983**, *130*, 134.
(22) Frieden, C. *Trends Biochem. Sci.* **1993**, *18*, 58−60.
(23) Frieden, C. *Methods Enzymol.* **1994**, *240*, 311−322.
(24) Wachsstock, D. H.; Pollard, T. D. *Biophys. J.* **1994**, *67*, 1260−1273.